Ring-Opening and Branching in Polycarbonates: A Density Functional-Monte Carlo Study

ARTICLE · MARCH 2005

DOI: 10.1021/bk-2005-0898.ch015

3 AUTHORS, INCLUDING:

Jaakko Akola

Tampere University of Technology

97 PUBLICATIONS **2,896** CITATIONS

SEE PROFILE

Ring-opening and Branching in Polycarbonates: a Density Functional/ Monte Carlo Study

R. O. Jones,[1] J. Akola,[1] and P. Ballone[1,2]

[1] **Institut für Festkörperforschung, FZ Jülich, D-52425 Jülich, Germany**
[2] **Dipartimento di Fisica, Università di Messina, I-98166 Messina, Italy**

Density functional calculations of the structures, potential energy surfaces, and reactivities for systems closely related to bisphenol A-polycarbonate (BPA-PC) provide the basis for a model describing the ring opening polymerization of its cyclic oligomers by nucleophilic molecules. The model comprises a fixed number of difunctional particles and harmonic bonds, and includes a low concentration ($0.01\% \leq c_a \leq 0.36\%$) of monofunctional active particles able to modify pattern of the bonds without changing the total number. Monte Carlo simulations using this model show that in 2D and 3D there is a transition from unpolymerized cyclic oligomers at low density to a system of linear chains at high density. Entropy in the distribution of inter-particle bonds drives chain formation. The effects of branching defects are investigated by adding trifunctional units (of concentration c_3). At sufficiently high density and c_3 values, the linking of polymer chains by trifunctional units gives rise to an aggregate (*gel*) incorporating most of the system mass.

Introduction

The outstanding mechanical, optical and thermal properties of polycarbonates underlie their diverse industrial applications, which motivate the continuing interest by experimental and computational research groups. Although polycarbonates have been produced on an industrial scale for decades, important questions remain concerning the relation between their macroscopic properties and the atomistic structure. An example is the polymerization of cyclic oligomers of bisphenol A polycarbonate (BPA-PC) to long chains and rings, whose size distribution is crucial to the thermal and mechanical properties. The linear structure of BPA-PC can be modified by branching centers arising from parasitic reactions, impurities, or additives. The resulting cross-links can alter greatly the polymer size distribution and the dynamical (e.g., diffusion, viscosity) and mechanical properties.[1,2]

Branching can also result in transitions to qualitatively new phases such as gels and rubber.[3]

A detailed understanding of the molecular size distribution and of the effects of branching requires a multifaceted investigation covering electronic and structural properties, chemical kinetics, and statistical mechanics. We describe here two examples of such computational investigations: the first explores the ring-opening polymerization (ROP) of BPA-PC starting from its cyclic oligomers and using small nucleophilic catalysts,[4] the second analyzes the influence of branching centers on the molecular structure and size distribution.

The basic reaction step leading to the ROP of BPA-PC has been investigated by combined density functional (DF)/ molecular dynamics computations,[5] which provide reliable predictions of reaction pathways and energies for these systems. The effect of many such reactions occurring in a condensed environment has then been investigated by Monte Carlo (MC) computations for a model based on the DF results, which provide key parameters. The model consists of structureless particles representing BPA monomers, with harmonic springs representing covalent bonds among them. It also includes catalyst particles and a bond interchange mechanism mimicking the reaction investigated by DF. The model describes fully flexible chains and rings, and thus provides an idealized view of BPA-PC. Moreover, our assumption of equilibrium polymerization allows us to use standard statistical mechanics approaches like MC, and to compare our results to those of previous studies for equilibrium ("living") polymers.[6]

The role of branching defects on the equilibrium structure has been investigated following the same strategy used to study polymerization. First, the chemical pathways leading to branching defects have been analyzed by DF computations.[7] The equilibrium properties of fluid mixtures of di- and trifunctional units have then been determined by Monte Carlo simulations as a function of density, temperature and concentration c_3 of the trifunctional monomers. Whenever the density and c_3 concentration are sufficiently high, the linking of polymer chains leads in 2D and 3D to a molecular aggregate (gel) comprising most of the system mass. This is a continuous transition analogous to percolation.

Reactions of phenoxides with cyclic tetramer

The ring-opening polymerization of cyclic oligomers of BPA-PC is catalyzed by nucleophilic molecules such as lithium and sodium phenoxide (LiOPh and NaOPh, respectively). The reactions have remarkably low exotherms, with enthalpy changes at the limit of the experimental resolution ($\Delta H \leq 0.3$ kcal/mol in the case of LiOPh).[8] Our DF calculations of the cyclic BPA-PC tetramer have shown that the local coordination of this molecule is very similar to that in the PC chains, and its reaction with LiOPh and NaOPh follows the path illustrated in Fig. 1.[9] An attack involving the (positively charged) metal atom is most likely at

the carbonate group, as confirmed by experimental studies on a number of functionalized bisphenols using a variety of catalysts.[10] Therefore, we have performed a constrained simulation using the distance R_C between the carbonyl C and the reactant O as the initial reaction coordinate.

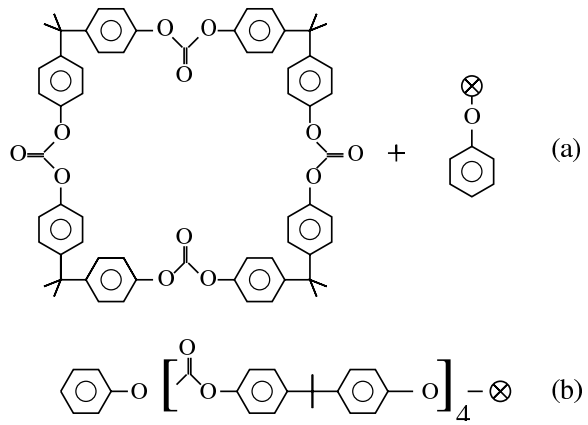

Figure 1. Schematic view of the first step in the ring opening polymerization of BPA-PC. The active site is an electropositive metal atom, identified by a cross.

Fig. 2 shows six snapshots of the trajectory for the reaction of LiOPh approaching from outside the cyclic tetramer.[9] The reactants interact weakly for $R_C \sim 4$, with steric hindrances from neighboring phenyl rings giving rise to an energy barrier of 4 kcal/mol at $R_C = 3.8$ Å. For shorter separations, the Li-O attraction induces a rotation of the carbonyl group and a rapid decrease (~ 15 kcal/mol) in the potential energy [2(2)]. Smaller values of R_C lead to a C atom surrounded by four O atoms with approximately tetrahedral coordination [2(3)]. A reduction of R_C to 1.5Å (corresponding to a second energy barrier of 4 kcal/mol) breaks the symmetric bonding of Li, and the Li is now attached to the tetrahedral O bound to a single C atom [2(4)]. This bond provides a 3-fold axis for rotations of the O-Li bond that result in very small energy variations.

Under normal thermodynamic conditions, the O-Li bond can then be oriented with equal probability along three directions. One relaxation gives rise to structure 2(6), which has a weak bond between Li and the new carbonyl O. This bond will break at room temperature, leading to the open chain with an active -C-O-Li termination. This configuration has essentially the same potential energy as the original reactants, in agreement with experimental evidence. Moreover, the chain termination reproduces the structure and chemical characteristics of the original LiOPh.

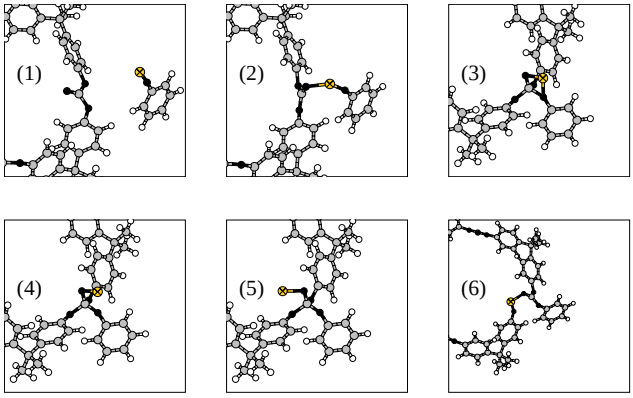

Figure 2. Reaction of LiOPh with cyclic tetramer of BPA-PC. The product (6) is a Li-terminated chain (Li atom crossed). Only part of the chain is shown.

It could catalyze the ring opening of further oligomers, giving rise to a "living polymer". The extension of these computations to different reagent (diphenyl carbonate) and catalyst (tetraphenylphosphonium phenoxide) molecules[11] shows that the energy barrier and the energy difference between reagents and products can be tuned by an appropriate choice of the chemical species.

Additional DF results on the structure, energy and vibrational properties for molecules related to bisphenol carbonate (from saturated fragments to cyclic oligomers of up to four BPA monomers)[12] can be summarized as follows: structural and vibrational properties of covalent bonds are highly transferable from one BPA aggregate to another. The structures of cyclic dimer and trimer are strained, but the cyclic tetramer is remarkably strain-free and displays structural features similar to those of extended chains. Total energies and vibrational entropy *per monomer* should then depend weakly on the molecular weight above three monomers, provided the rearrangements do not change the number and type of bonds. The DF results for structure, energy and vibrational frequencies agree well with available experimental data.

Polymerization of PC: Model simulations

The analysis of the reaction between the cyclic tetramer and LiOPh and NaOPh clarifies the origin of their catalytic activity, and provides much information about the reaction mechanisms. However, it does not explain why cyclic oligomers polymerize under appropriate conditions, since reactants and products have nearly the

same potential energy. The vibrational properties that determine configurational entropy contributions also change little during the reaction. In addition, translational entropy (accounting for the ideal part of $S(T)$) favors a multitude of small molecules over a few large connected aggregates.

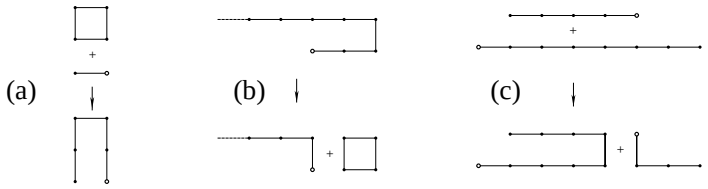

Figure 3. Model used to study polymerization: (a) chain formation from ring, (b) ring formation from chain, and (c) tail interchange between active chains. The active site is denoted by an open circle.

The polymerization process has been studied using a model, in which BPA-PC structural units are represented by Lennard-Jones (LJ) particles connected by harmonic springs representing the covalent bonds in the polymer backbone.[13,14] Each particle forms one or two bonds, so that the system comprises open chains and rings without branching, and the catalyst is represented by *active* particles that can interchange bonds with a neighboring particle. The active particles can form only one bond, so that they must be at an end of a chain with at least two particles.

The rules for bond interchange are shown in Fig. 3, which illustrates the basic processes taking place: the incorporation [3(a)] and the separation [3(b)] of a ring from an open chain carrying an active head, and the interchange of segments between chains [3(c)]. Constant volume Monte Carlo simulations are performed by sampling the positions and bonding configuration using a Metropolis algorithm.

We have investigated systems in 2D and 3D over a wide range of densities and temperatures, focusing on the limit of low catalyst concentration (from 0.01 to 0.36 %). All computations were started by equilibrating a sample of 2500 cyclic tetramers before introducing a small number (from 1 to 36) of dimers, each with one active particle representing the metal termination of the M-OPh molecule. The primary role of the catalyst is to enhance the kinetics of the rearrangement of the covalent bonds. However, since the number of bonds is conserved during ring-opening polymerization of BPA-PC, the number of catalyst molecules also determines the number of free chain terminations (active or not), which is conserved during the polymerization process. We express densities in terms of the packing fraction η, defined as $\eta = \pi\rho\sigma^2/4$ and $\eta = \pi\rho\sigma^3/6$ in 2D and in 3D, respectively, where σ is the Lennard-Jones diameter of our particles. Energies and

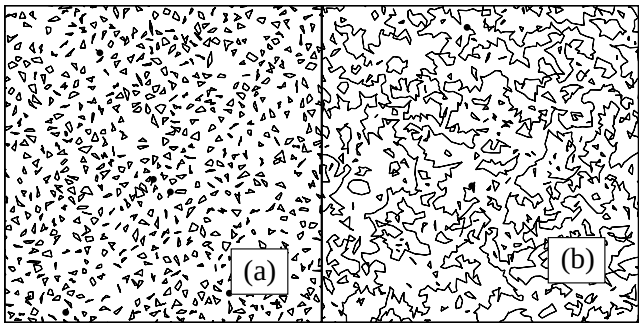

Figure 4. Snapshots of (a) the initial tetramer fluid, and (b) a configuration at equilibrium under the bond interchange mechanism. Simulation in 2D at $\eta = 0.4$ and $T = 3$. Solid dots identify active particles.

temperatures are measured in units of the LJ energy parameter ϵ. A temperature of $T = 3$ corresponds to 375 K for a typical molecular system with $\epsilon = 0.25$.

The addition of the catalyst influences the configuration dramatically in most cases, leading to long open chains with up to ~ 50 % of the particles (see Fig. 4). The remaining particles are subdivided into an equilibrium population of rings, whose average size is much smaller than that of the chains.

We first discuss the results in 2D, which are less affected by finite-size effects than their 3D counterparts with the same particle number. In Fig. 5 we show the average length of the active chain N_a as a function of density for different concentrations of active particles. The degree of polymerization increases with increasing density, with a sharp rise at $\eta \sim 0.15$. The competition between active chains for the available monomers means that the average chain length decreases with increasing concentration of the active particles. The increasing average length with decreasing N_a makes the rise at $\eta = 0.15$ more pronounced, leading to a discontinuous transition in the limit of vanishing catalyst concentration.[13]

The equilibrium size distributions of rings and chains are characterized by the mass-fraction distributions $P_r(L)$ and $P_l(L)$, defined as the percentage of monomers belonging to a ring or a chain, respectively, of length L. The Zimm-Schulz distribution:

$$P_l(L) \propto L^\gamma \exp\left[-\gamma L/\langle L_l \rangle\right] \tag{1}$$

provides a fair fit to all curves, with an exponent ($1.1 < \gamma < 1.4$) close to the value predicted by analytic theories $\gamma = 43/32$.[15] This fit may reflect simply the existence of a unimodal, broad, and relatively featureless $P_l(L)$ that decays exponentially for high L and scales simply with η and c_a. A similar

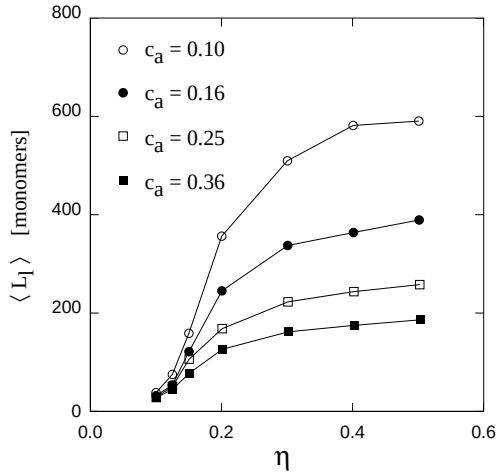

Figure 5. Average length of active chains as a function of packing fraction η for different concentrations (%) of active particles. Simulations in 2D [Ref. 14(a)].

fit is provided by other expressions, including $P_l(L) \propto L \exp\left[-\gamma L/\langle L_l \rangle\right]$ and $P_l(L) \propto L^{\gamma} \exp\left[-L/\langle L_l \rangle\right]$). The distribution $P_r(L)$ for rings changes little over the range of η and c_a considered in our simulations.

Temperature also affects the average length of the chains, although less dramatically than the density. The monotonic rise of the polymerization degree with increasing T indicates that entropy is the driving force stabilizing the long chains. This is supported by the behavior of the average potential energy, which rises steadily during polymerization. Since the spontaneous evolution of every system is towards a state of lower free energy, the rise of the average potential energy per particle $\langle U \rangle$ must be over-compensated by the simultaneous increase of the system entropy. Moreover, the positive sign of both the potential energy and entropy changes upon polymerization ($\Delta U > 0$, $\Delta S > 0$) implies that the model displays a floor temperature T_f separating an unpolymerized phase (at $T < T_f$) from the polymerized phase at $T > T_f$. We have not observed the transition directly, because it appears to occur below the temperature range accessible to our simulations, which require a sufficiently fast relaxation of the bonding configurations to reach equilibrium.

The simulations in 3D and 2D show both similarities and differences. The tendency to polymerize is much stronger in 3D, with the average mass of the active chain generally being well above 80 % of the total, and the polymerization line occurs in 3D at a packing fraction an order of magnitude lower (see Fig. 6).

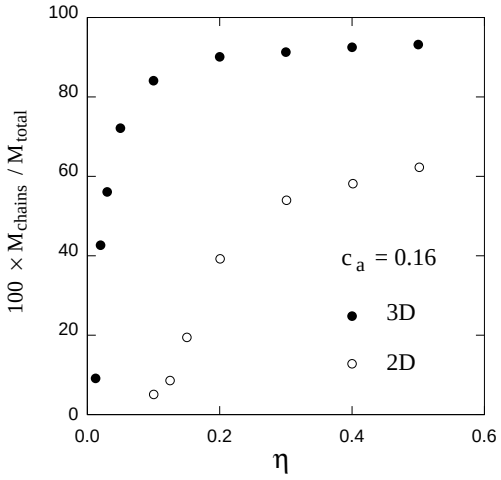

Figure 6. Fraction of system mass in open chains in 2D and 3D as a function of packing fraction η [Ref. 14(a)].

The degree of polymerization in 3D decreases slightly but monotonically with decreasing T, as found in 2D. At $\eta = 0.3$ and $c_a = 0.16\%$, for example, open chains account for 91.3% of the total mass for $T = 3$, decreasing to 84.8% at $T = 0.6$. We did not observe a polymerization transition on changing T alone, so that the polymerization line in the $\eta - T$ plane must be a very steep function of η. In both 2D and 3D there is a systematic and significant increase of viscosity and a decrease in diffusion during polymerization.

Branching and polymerization in polycarbonates

The model discussed above has been extended by introducing LJ particles that form three bonds and give rise to branching, and Fig. 7 shows an example in the polycarbonate context.[2] The course of the reaction depends on density, T, and the concentration of additives and impurities, and the resultant polymer shows a shear sensitivity that is directly related to the amount of branching agent and inversely related to the amount of the initiator. As in our previous simulations, a low concentration c_a of active particles allows equilibration with respect to the bond configuration. The model emphasizes the role of entropy over potential energy, since all particles interact by the same LJ potential, all bonds are equivalent, and their number is conserved. We have performed simulations in 2D and 3D for concentrations of trifunctional units c_3 from 0.1 % to 32 % and densities covering the

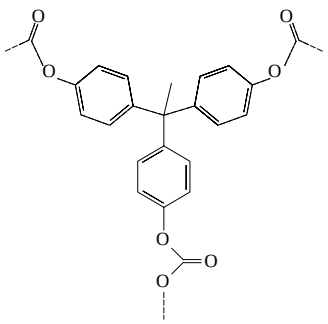

Figure 7. Schematic view of the branching center in bisphenol-A polycarbonate produced by the ring-opening polymerization of cyclic oligomers in the presence of small amounts of 1,1,1-tris(4-hydroxyphenyl)ethane, THPE [Ref. 14(b)].

polymerization line found for $c_3 = 0$. Only the lowest range of c_3 (up to a few percent) is relevant for industrial applications, but a much wider interval has been explored for completeness.

Aggregates with trifunctional units (see Fig. 8(a)) are much more compact than linear polymers of comparable size (see Fig. 8(b)), if other parameters (η, T, c_a and dimensionality) are equal. The reduced gyration radius affects, the dynamical and mechanical properties and the stability of large aggregates, since compact molecules carrying active heads are more likely to self-mutilate [Fig. 3(b)] than extended chains. This tends to reduce the average molecular weight, thus partially compensating the trend towards larger aggregates due to the linking of polymeric segments by trifunctional units. A more quantitative analysis of these effects is provided by monitoring the size distribution and the average size of molecules with one or more chain terminations ($\langle L_l \rangle$) or at least one trifunctional unit ($\langle L_3 \rangle$). These account for a large fraction of the total mass in the polymeric phase, and the analysis of either provides similar information.

Polymerization and gel transition in 2D

Simulations for 2D systems with $c_3 = 0$ showed[13,14] that the polymeric phase is stable if $\eta \geq 0.16$, and intuition suggests that introducing a small number of trifunctional units could enhance polymerization by allowing the formation of interchain links and aggregates of chain segments. For 2D systems with $c_3 \sim 0.1 - 1$ %, however, the addition of trifunctional particles *lowers* the degree of polymerization significantly, resulting in a sizable reduction of the average size $\langle L_l \rangle$ for molecules with at least one chain termination. The apparent trend towards smaller aggregates is due to the reduction in the molecular extension by branching

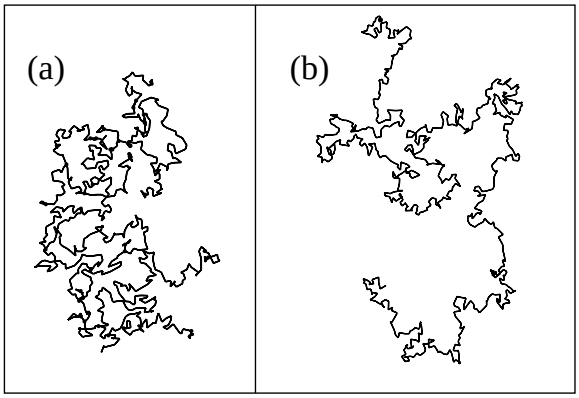

Figure 8. Typical molecular structures in 2D simulations at $\eta = 0.3$, $T = 3$ *and* $c_a = 0.16\%$. *(a)* $c_3 = 4\%$ *; (b)* $c_3 = 0$.

centers described in the previous section. In 2D this decrease of polymerization upon addition of trifunctional units is a major effect, and only large concentrations of trifunctional units are able to reverse the depolymerization trend. Increasing further the c_3 concentration results in a new (gel) phase qualitatively different from the polymer found for $c_3 = 0$. The new phase is formed across a phase transition, which, together with the polymerization transition found previously,[13,14] allows us to identify three distinct phases for the model: a fluid phase comprising oligomers; a gel, in which most of the mass is included in a single molecule; and a polymeric phase comprising several linear or branched aggregates of fairly large ($L \geq 100$ monomers) size. The gel forms via a continuous transition with increasing c_3, resulting from the linking of aggregates with a wide range of sizes. The accompanying anomalous increase of size fluctuations supports both the continuous nature of the phase transformation and the connection to percolation.

Fig. 9 shows $P_l(L)$ for samples at $\eta = 0.5$, $T = 3$ and c_3 values covering the gel transition ($c_3 \sim 10\%$ for these conditions). In the absence of branching,[14] $P_l(L)$ is approximated well by the Zimm-Schulz function $\propto L^\gamma \exp[-\gamma L/\langle L\rangle]$, with an exponent γ close to the value ($\gamma = 43/32$)[15] for a model closely related to the present one.

The addition of branching centers affects $P_l(L)$ significantly for low c_3, as indicated by the rapid decrease of $\langle L_l\rangle$ close to $c_3 = 0$: the peak of $P_l(L)$ moves towards lower sizes, while the tail of the distribution extends to higher sizes. The distribution deviates significantly from the Zimm-Schulz form, and an exponential form [$P_l(L) \propto \exp[-\alpha L/\langle L\rangle]$, $\alpha \sim 0.36$] is more appropriate in the c_3 range corresponding to a lower degree of polymerization (see the curve for $c_3 = 1\%$

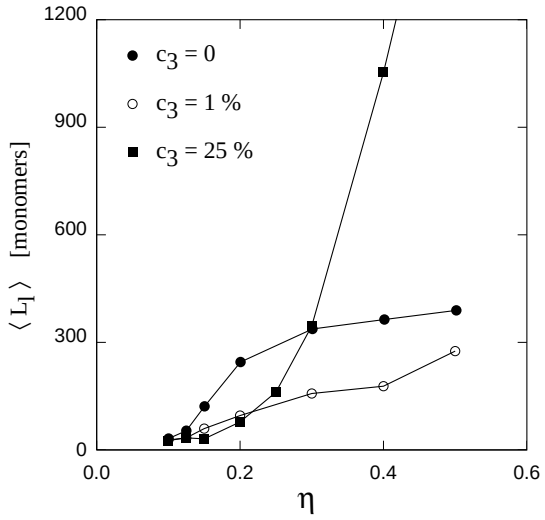

Figure 9. $\langle L_l \rangle$ *as a function of* η *at three values of* c_3 *[Ref. 14(b)].*

in Fig. 10). $P_l(L)$ is bimodal in the gel, with the high-L peak centered at sizes ($L \sim 9000$ monomers) close to the total sample size (see the curve for $c_3 = 25\%$ in Fig. 10). At the gel transition ($c_3 = 10\%$), $P_l(L)$ is nearly constant over a wide size range, which explains the large fluctuations in $\langle L_l \rangle$.

Polymerization and gel transition in 3D

Many features observed in 2D systems are found in 3D, although the greater stability of the 3D polymer phase influences the properties of branched systems. The reduction of $\langle L_l \rangle$ at low c_3 is much less pronounced than in 2D, although it is evident in the c_3 dependence of $\langle L_l \rangle$. The rapid rise of $\langle L_l \rangle$ at higher c_3 values is accompanied by a large increase in the size fluctuations, which allows us to locate the gel transition at $c_3 \sim 2$ % for these conditions of density and T.

The dependence of the molecular size distribution $P_l(L)$ on density and c_3 in 3D samples is greater than in 2D, reflecting the increased stability of both polymer and gel. Starting from a $P_l(L) \propto L \exp[-L/\langle L \rangle]$ for $c_3 = 0$, the addition of only $0.1-0.2\%$ of trifunctional particles changes significantly the shape of $P_l(L)$, which is now approximated better by $P_l(L) \propto \exp[-\alpha L/\langle L \rangle]$ ($\alpha \sim 0.3$). With increasing c_3, the height and the width of the first $P_l(L)$ peak decrease monotonically, while the large-L tail develops into a secondary peak at $L \sim 6000$ for $c_3 \sim 1\%$. At the gel point ($c_3 = 2\%$), identified here by the maximum in the

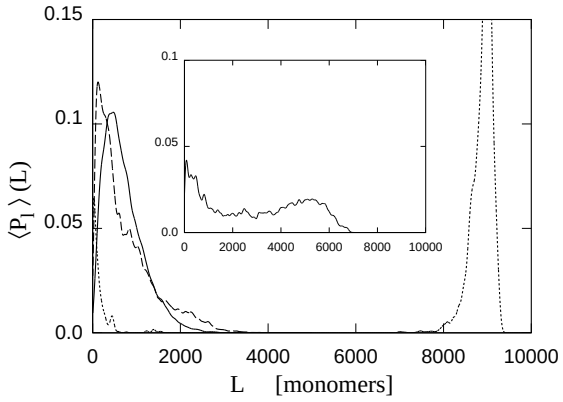

Figure 10. Mass fraction distribution $\langle P_l \rangle$ in 2D samples at $\eta = 0.5$ and $T = 3$. Full line: $c_3 = 0$; dashed line: $c_3 = 1\%$; dotted line: $c_3 = 25\%$. Inset: $c_3 = 10\%$, corresponding to the gel point [Ref. 14(b)].

relative size fluctuations, $P_l(L)$ is clearly bimodal. For larger values of c_3, most of the weight under the $P_l(L)$ curve belongs to the high-L peak, which moves towards larger sizes (saturating at $L \sim 9000$) and reduces its width.

As discussed above, the polymerization and gel transitions are driven by the entropy associated to the bonding configuration, and this is emphasized by the fact that polymerization becomes weaker with decreasing T. The analysis of snapshots, the mass-fraction distribution $\langle P_l(L) \rangle$, and the molecular size fluctuations all show the progressive loss of gel characteristics as T is lowered, and the gradual evolution of these properties with changing T prevents the precise determination of the transition point. The polymerization and gel transitions are less sensitive to temperature in 3D than in 2D, mainly because the relevant range of c_3 is lower.

Discussion and Concluding Remarks

A combination of DF computations and MC simulations has been used to investigate ring-opening polymerization in BPA-PC. Density functional calculations have been used to determine the energy balance, the energy barrier and the path for the basic reaction leading to polymerization. The results show that reactants and products have nearly the same energy, and the potential energy barrier is low when the reaction is catalyzed by LiOPh, and vanishes in the case of NaOPh. Vibrational properties do not change significantly, so that the vibrational entropy is nearly unchanged by the reaction. A model incorporating these ingredients and

energy parameters from the DF computations has been devised: BPA-PC structural units are represented by Lennard-Jones particles, and the covalent bonds in the polymer backbone are described by harmonic springs. Each particle forms one or two harmonic bonds, so that the system comprises open chains or rings without branching. The reaction is initiated by introducing a small number of *active* particles. These interact with the rest of the system via the same potentials as the other particles, but they mimic the behavior of the catalytic head in MOPh because (a) they form one and only one bond, and (b) bond exchanges occur only when at least one of the bonds involves an active particle.

Extensive MC simulations show that the model displays a strong tendency to form long chains that is enhanced by increasing density, temperature and dimensionality. Simple thermodynamic considerations show that the driving force towards polymerization is provided by the entropy of the bonding configuration, whose contribution to free energy rises with increasing temperature.

The role of branching defects has been investigated by including trifunctional monomers in the model used to study polymerization, and equilibrating the structure and bond configuration by MC simulations. The addition of trifunctional particles displaces the polymerization line and introduces a qualitatively new (*gel*) phase. Simulations have been performed here for 2D and 3D systems. In 2D systems the effect of branching centers on the molecular size distribution is different at low and high concentrations. At low concentrations the main effect is to reduce the gyration radius of the molecule, which limits the size of the aggregates. At densities slightly above the polymerization line the system may revert to the unpolymerized state over a wide range of c_3. At high c_3 and in the polymer range of (η, T), the linking of chains by trifunctional units increases the molecular size and leads to a gel at a critical concentration that depends on η, T, and dimensionality.

Most results for 2D systems remain qualitatively valid in 3D. Small concentrations of trivalent particles lower the degree of polymerization at densities $0.04 \leq \eta \leq 0.15$, although this effect is less important than in 3D and is not seen for $\eta \geq 0.15$. Higher concentrations of trifunctional particles lead to a continuous transition to a gel, which occurs with increasing c_3 and packing fraction η. The evolution of the size distribution with increasing c_3 is similar in 2D and in 3D.

Lowering T reduces the degree of polymerization even in the absence of branching, and trifunctional particles enhance greatly the sensitivity to temperature of both polymer and gel. The latter is affected more, and we observe a reversible transition between the polymer at low T and the gel at high T, for 2D samples at high density and high values of c_3. The continuous nature of the transition hampers the determination of the transition point in this case. The effect of decreasing T is reduced in 3D for the range of c_3 studied here, although similar effects to those observed in 2D could also occur for larger values of c_3. The changes in the system properties with changing temperature and density are fully reversible.

The calculations were performed in the FZ Jülich on a Compaq DS20E server and XP1000 workstations provided in part by the Bundesministerium für Bildung und Wissenschaft, Bonn, within the MaTech-Kompetenzzentrum "Werkstoffmodellierung" (03N6015). We thank D. Brunelle (G.E., Niskayuna, NY), S. Greer (University of Maryland, College Park, MD), and F. Bruder, S. Kratschmer, and M. Möthrath (Bayer AG, Krefeld, Germany) for helpful discussions.

References

1. See, for example, Clarke, S. M.; Hotta, A.; Tajbakhsh, A. R.; Terenjev, E. M. *Phys. Rev. E* **2001**, *64*, 061702.
2. Krabbenhoft, H. O.; Boden, E. P. *Makromol. Chem., Macromol. Symp.* **1991**, *42/43*, 167. Branching increases heat resistance and shear sensitivity.
3. de Gennes, P. G. *Scaling concepts in Polymer Physics*, Cornell University Press: Ithaca, 1979.
4. Brunelle, D. J. in: *Ring-opening Polymerization: Mechanisms, Catalysis, Structure, Utility*, Brunelle, D. J., Ed.; Hanser: München, Germany, 1993, pp. 1 and 309.
5. Car, R.; Parrinello, M. *Phys. Rev. Lett.* **1985**, *55*, 2471. We have used the CPMD program version 3.0, Hutter, J. *et al.*, Max-Planck-Institut für Festkörperforschung and IBM Research 1990-99.
6. For comprehensive reviews, see Greer, S. G. *Adv. Chem. Phys.* **1996**, *94*, 261; Greer, S. C. *J. Phys. Chem. B* **1998**, *102*, 5413; Greer, S. C. *Annu. Rev. Phys. Chem.* **2002**, *53*, 173.
7. Akola, J.; Jones, R. O. *Macromolecules* **2003**, *36*, 1355.
8. Brunelle, D. J.; Boden, E. P.; Shannon, T. G. *J. Am. Chem. Soc.* **1990**, *112*, 2399.
9. Ballone, P.; Montanari, B.; Jones, R. O. *J. Phys. Chem. A* **2000**, *104* 2793.
10. Brunelle, D. J.; Shannon, T. G. *Makromol. Chem., Macromol. Symp.* **1991**, *42/43* 155.
11. Ballone, P.; Jones, R. O. *J. Phys. Chem. A* **2001**, *105*, 3008.
12. Montanari, B.; Ballone, P.; Jones, R. O. *J. Chem. Phys.* **1998**, *108*, 6947; Montanari, B.; Ballone, P.; Jones, R. O. *Macromolecules* **1998**, *31*, 7784; Ballone, P.; Montanari, B.; Jones, R. O.; Hahn, O. *J. Phys. Chem. A* **1999**, *103*, 5387; Montanari, B.; Ballone, P.; Jones, R. O. *Macromolecules* **1999**, *32*, 3396.
13. Ballone, P.; Jones, R. O. *J. Chem. Phys.* **2001**, *115*, 3895.
14. (a) Ballone, P.; Jones, R. O. *J. Chem. Phys.* **2002**, *116*, 7724, (b) *ibid.* **2002**, *117*, 6841.
15. Schäfer, L. *Phys. Rev. B* **1992**, *46*, 6061; Gujrati, P. D. *Phys. Rev. B* **1989**, *40*, 5140.